Eur. Phys. J. C (2018) 78:15
https://doi.org/10.1140/epjc/s10052-017-5499-9

THE EUROPEAN PHYSICAL JOURNAL C

Regular Article - Experimental Physics

Mitigation of ^{42}Ar/^{42}K background for the GERDA Phase II experiment

A. Lubashevskiy[1,2,a], **M. Agostini**[3], **D. Budjáš**[4], **A. Gangapshev**[1,5], **K. Gusev**[2,4,6], **M. Heisel**[1], **A. Klimenko**[1,2], **A. Lazzaro**[4], **B. Lehnert**[7,10], **K. Pelczar**[8,11], **S. Schönert**[4], **A. Smolnikov**[1,2], **M. Walter**[9], **G. Zuzel**[8]

[1] Max Planck Institut für Kernphysik, Heidelberg, Germany
[2] Joint Institute for Nuclear Research, Dubna, Russia
[3] Gran Sasso Science Institute, L'Aquila, Italy
[4] Physik Department E15, Technische Universität München, Munich, Germany
[5] Institute for Nuclear Research of the Russian Academy of Sciences, Moscow, Russia
[6] Russian Research Center Kurchatov Institute, Moscow, Russia
[7] Institut für Kern- und Teilchenphysik Technische Universität Dresden, Dresden, Germany
[8] Institute of Physics, Jagellonian University, Cracow, Poland
[9] Physik Institut der Universität Zürich, Zurich, Switzerland
[10] Present address: Physics Department, Carleton University, Ottawa, Canada
[11] Present address: INFN Laboratori Nazionali del Gran Sasso, LNGS, Assergi, Italy

Received: 2 August 2017 / Accepted: 21 December 2017 / Published online: 11 January 2018

Abstract Background coming from the ^{42}Ar decay chain is considered to be one of the most relevant for the GERDA experiment, which searches for the neutrinoless double beta decay of ^{76}Ge. The sensitivity strongly relies on the absence of background around the Q-value of the decay. Background coming from ^{42}K, a progeny of ^{42}Ar, can contribute to that background via electrons from the continuous spectrum with an endpoint at 3.5 MeV. Research and development on the suppression methods targeting this source of background were performed at the low-background test facility LArGe . It was demonstrated that by reducing ^{42}K ion collection on the surfaces of the broad energy germanium detectors in combination with pulse shape discrimination techniques and an argon scintillation veto, it is possible to suppress ^{42}K background by three orders of magnitude. This is sufficient for Phase II of the GERDA experiment.

1 Introduction

In GERDA bare germanium diodes immersed in liquid argon (LAr) are used both as a source and the detector of the neutrinoless double beta ($0\nu\beta\beta$) decay of ^{76}Ge [1]. Broad Energy Germanium (BEGe) detectors [2] were introduced to GERDA in Phase I and dominate the Phase II detector inventory. BEGe detectors have better energy resolution and a significantly thinner dead layer than semi-coaxial detectors [3]. The latter makes them prone to surface events from the beta particles, which can penetrate the dead layer. This kind of background is considered to be one of the most dangerous in GERDA Phase II.

Liquid argon simultaneously serves as a detector coolant and as passive shielding against external radiation. In addition, some backgrounds can be suppressed efficiently by a LAr veto detecting scintillation light generated by background events in the liquid argon. However, cosmogenic ^{42}Ar poses an additional source of background. It is present in natural argon and decays into ^{42}K. ^{42}K is a beta emitter (Q_β= 3525 keV) with a half-life of 12.3 h (see Fig. 1). The region of interest (ROI) of the $0\nu\beta\beta$ decay is centered around $Q_{\beta\beta}$= 2039 keV [4]. High energy electrons ($E \geq Q_{\beta\beta}$) from ^{42}K beta decays, occurring very close to the detector surface, can increase the background level in the ROI.

During the first commissioning runs of GERDA Phase I it was found that the intensity of the 1525 keV gamma line from ^{42}K is much higher than expected from a homogeneous distribution of ^{42}Ar, assuming a natural abundance of < 41 µBq/kg [6].[1] A similar conclusion emerged from the measurements in the LArGe test facility [8], operated in the framework of GERDA. The measurements [3] show that the enhancement of ^{42}K background can be attributed to an accumulation effect: after the decay of their mother isotope, ^{42}K ions retain their positive charge long enough to move in the electric field of the germanium detectors [9]. Consequently,

[a] e-mail: lav@nusun.jinr.ru

[1] Later this limit was reconsidered [7] and changed to 92^{+22}_{-46} µBq/kg.

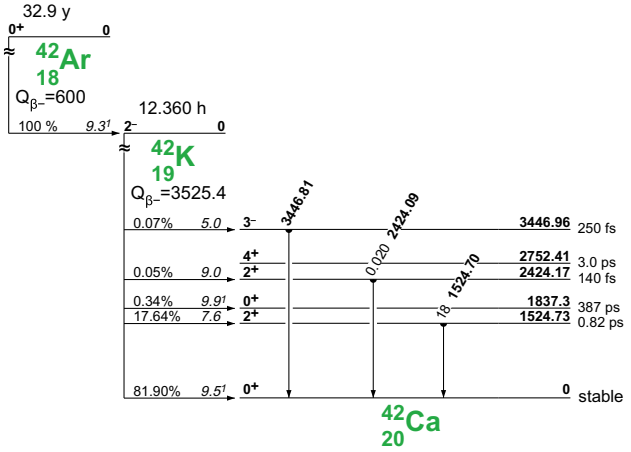

Fig. 1 Simplified decay scheme of ^{42}Ar [5]. The 1525 keV gamma line is used to identify ^{42}K

^{42}K ions are attracted towards the germanium detectors and their distribution in liquid argon becomes inhomogeneous.

The background contribution coming from the ^{42}Ar decay chain was considerably suppressed in GERDA Phase I by enclosing each detector string with a grounded cylinder made from 60 µm copper foil (called mini-shroud, MS) [1]. The mini-shroud screens the electric field of the germanium detectors and creates a mechanical barrier preventing collection of the ^{42}K ions on detector surfaces and thus decreasing the ^{42}K background level.

However, the copper MS is not a viable option for Phase II: the main reason is that argon scintillation light generated inside the copper MS would be blocked from detection by the LAr veto, thus the veto efficiency would be seriously impaired. Another reason is that the radiopurity of the copper MS used in GERDA Phase I does not suffice the more stringent radiopurity requirements of Phase II. Therefore, it was decided to develop a new mini-shroud. Results from this development and detailed tests of its ^{42}Ar mitigation capability are described here. In addition, BEGe detectors have powerful pulse shape discrimination (PSD) capability which allows to mitigate surface events from β-decays of ^{42}K. The suppression capability of ^{42}K background events by PSD has been included in this investigation. The suppression factors (SF) of passive and active methods obtained in the LArGe test stand are presented, as well as estimates for ^{42}K suppression in the GERDA Phase II environment.

2 Experimental

2.1 Development of a transparent mini-shroud

^{42}K background can be suppressed e.g. by modifying the electric field produced by the high voltage applied to detectors, or by a mechanical barrier. Several solutions were tested for GERDA (mini-shroud made of copper mesh, copper plate, plastic scintillator, etc.) and proved to work well in liquid argon. The solution described here is the mini-shroud made from a transparent plastic foil. It shows the best combination of properties beneficial for ^{42}K mitigation, namely background suppression, high radiopurity, having no detrimental impact on the LAr veto etc. The MS does not screen the E-field of the detector, but as a mechanical barrier for ^{42}K ions prevents their drift towards the germanium detector. The mini-shroud encapsulates the detector, but is not tight to prevent liquid argon from pouring inside during the detector immersion. The collected ^{42}K atoms decay on the foil's surface at a distance of several millimeters from the detector, thus beta particles are attenuated by liquid argon.

A thin nylon film (thickness 125 µm) was chosen as the construction material. It is robust, durable and flexible. It has good transparency for the visible light and exhibits a very low intrinsic radioactivity. Several pieces of nylon film were provided by Princeton University. These are left-overs from the material used in Borexino to construct the Inner Vessel [10]. The radioactive impurities are only 2 ppt for ^{238}U and 4 ppt for ^{232}Th [11].

Scintillation light emitted by liquid argon (128 nm wavelength) must be converted to wavelengths suitable for scintillation light detectors (e.g. sensitive range of PMTs is 250–500 nm). Thus the nylon mini-shroud (NMS) was covered with a wavelength shifter (WLS). It allows light to pass through the nylon film as it is opaque for deep ultraviolet radiation below 300 nm. The performance of the WLS coating, its robustness and stability in time were also investigated in various tests. These studies include an optimization of the composition and thickness of the WLS coating.

The performance of the WLS coating was tested with an UV spectrophotometer (Cary Eclipse) at the Max-Planck-Institut für Kernphysik (MPIK) in Heidelberg. Direct investigation of the shifting of argon scintillation light at 128 nm was not possible since no light source in this far UV region was available. Instead, a qualitative comparison was made with the emission light of the spectrophotometer at 200 nm.

The initial WLS solution was prepared by dissolving 1,1,4,4-tetraphenyl-1,3-butadiene (TPB) [12] with polystyrene (PS) in a ratio of 1:10 in toluene (recipe previously used for coating of the VM2000 reflection foil in LArGe [13]). To improve the performance of the nylon mini-shroud we increased the concentration of TPB and replaced toluene by dichloromethane (DCM), the latter of which is used for the production of the reflector foils in GERDA Phase II [14]. A higher concentration of TPB in the polystyrene matrix increases the intensity of emitted light (see Fig. 2). However, too high TPB concentration decreases the mechanical stability of the coating. Finally, a TPB concentration in the range of 30–40% in the polystyrene matrix proved to be a good bal-

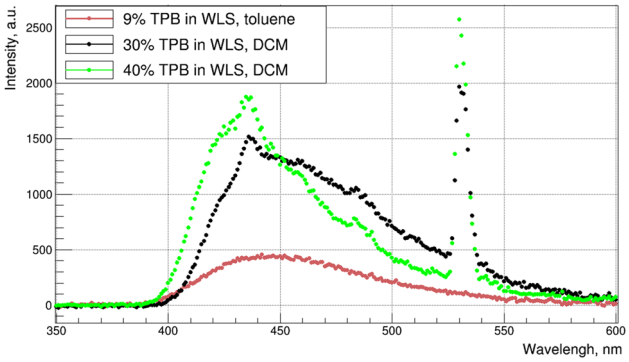

Fig. 2 Fluorescence spectra of the coated nylon samples with different composition of WLS measured with a Cary Eclipse UV spectrophotometer. The peak at 530 nm is a light contamination presumably from the excitation beam

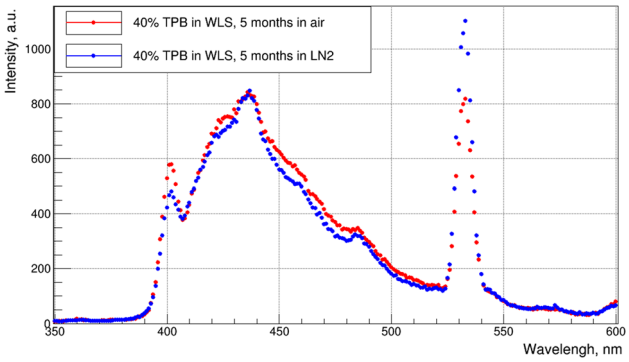

Fig. 3 Fluorescence spectra of the coated nylon samples stored in liquid nitrogen for 5 months (blue) and in air (red). The intensity scale is not comparable to that of Fig. 2. Since a lattice is used as an analyser, a scattering peak at double wavelength of the excitation beam of 400 nm is visible, as well as a contamination at 530 nm

ance between mechanical stability and light emission efficiency. The coating was applied by brushing both sides of nylon samples. The amount of deposited WLS (TPB with PS) is typically 0.3 mg per 1 cm^2, as estimated by weighting the nylon before and after coating.

Various tests were performed in order to understand the usability of such a foil in GERDA. Immersion of the nylon film in liquid nitrogen showed that it keeps flexibility at low temperatures and does not become brittle even after several weeks spent in cryogenic liquid. Long term stability of the coated nylon foils was checked in liquid nitrogen (5 months) and liquid argon (2 months in the LArGe cryostat). No visible deterioration of the coated surfaces was found. Changes in optical properties of the WLS were checked with the UV spectrophotometer. Figure 3 shows a comparison of samples kept in liquid nitrogen (blue dots) and in air (red dots) for 5 months each. No significant difference between the two fluorescence spectra was observed.

To construct the NMS fully covering the detector (or a string of detectors) it is necessary to connect several nylon

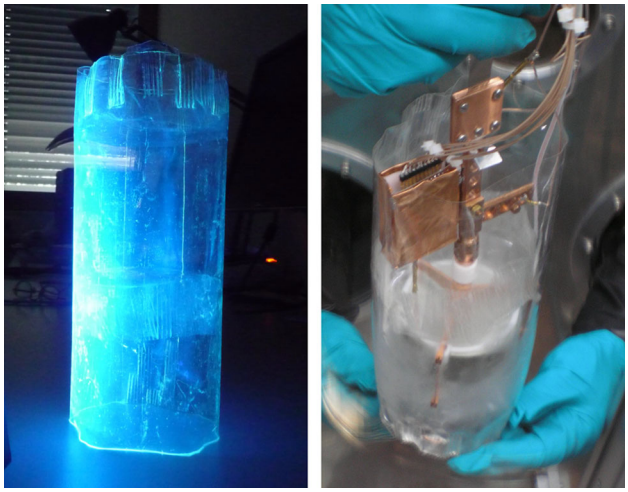

Fig. 4 Left: photo of the first version of a nylon mini-shroud coated with WLS (the photos were taken in UV light). The nylon sheets were connected by welding. Right: NMS in assembly with a bare BEGe detector inside the lock of LArGe

sheets together to form a cylindrical shape. Such connections should be radioactively clean and robust enough to survive manual handling and immersion into liquid argon. The first version of the mini-shroud was created by welding (see Fig. 4) not requiring any additional material, but the connections were brittle and easily damaged during handling.

Finally, nylon pieces were glued using a solution of resorcinol in ethanol and water with sodium meta-bisulphite [15]. It was confirmed that these connections are very robust and suitable for cryogenic operations. The glued NMS was placed around a dummy detector string (aluminum dummies of detectors and holders) and it was submerged in liquid nitrogen, showing that it is robust enough and can keep its shape during the slow immersion process (∼1 h) of the detector strings in GERDA. To minimize the risk of contamination, all preparations of the final shrouds for GERDA were performed in a clean room. Before the insertion into the GERDA cryostat, the detector array with the NMS and the LAr light instrumentation went through several outgassing cycles within the GERDA lock.

2.2 Contribution of the NMS to the GERDA background index

The content of radio-impurities of coated nylon films was checked by ICP-MS to verify that no significant background contribution is added to GERDA [16]. Results of the measurements are summarized in Table 1.
The difference in the radioactive contamination of the starting foil material and the aggregated contamination of the final NMS may have been caused by the impurities introduced during the preparation of the samples. The nylon cylinder for

Table 1 Radiopurity of the components of the NMS from ICP-MS measurements. Uncertainties are estimated to be about 30%. The upper limit is 90% C.L

Components	Mass per NMS (g)	U (ppt)	Th (ppt)
TPB	∼0.15	10	9
Polystyrene	∼0.34	< 5	10
Glue	–	< 10	< 10
Uncoated nylon	27.6	< 10	< 15
Coated nylon	21.5	11	18
Glued nylon	6.5	38	39
one NMS	28.1	6.1 µBq	2.6 µBq

each GERDA Phase II detector string typically has a height of 430 mm and a diameter of 103 mm. The mass of the NMS is about 28 g. We expect about 6.1 µBq of ^{238}U and about 2.6 µBq of ^{232}Th reside in a single NMS.

To prove that this radiopurity level is acceptable, a detailed simulation of the NMS background for the GERDA Phase II setup was performed. This Monte Carlo simulation is based on the MaGe framework [17] with the preliminary GERDA Phase II geometry, using seven detector strings with one NMS each, under the assumption of equilibrium in the U/Th chains [18]. It is necessary to note that the values were obtained assuming that daughter isotopes of ^{238}U and ^{232}Th do not escape from the NMS, otherwise the obtained results may be different. In particular, distribution of the activity due to the radon emanation is not discussed here since estimated activity in the NMS for GERDA is much smaller than other components inside the NMS, e.g. flat band cables [19]. The simulation code is validated with the GERDA calibration data. Radioactive isotopes were homogeneously distributed inside the NMS material. The simulated energy spectra of germanium detectors taken with ^{214}Bi and ^{208}Tl sources are shown in Fig. 5. Tracking of optical photons and the evaluation of the LAr veto suppression were only performed in the energy region of 1800–2300 keV, to save computation time. Suppression factors of 33±4 and ≥ 2000 are obtained for ^{214}Bi and ^{208}Tl, respectively. The large suppression is due to the thinness of the NMS, which allows the betas from ^{208}Tl and ^{214}Bi to escape the nylon and deposit a large fraction of their energy in the liquid argon. This creates a large scintillation signal which can be easily vetoed. The estimated contributions to the background index (BI) for ^{214}Bi are 1.8×10^{-4} cts/(keV kg year) before and 5.3×10^{-6} cts/(keV kg year) after applying the LAr veto. For ^{208}Tl these values are 2.7×10^{-4} cts/(keV kg year) and $< 1.4 \times 10^{-7}$ cts/(keV kg year) before, and after the LAr veto, respectively. The combination of these values gives the total contribution of the NMS to the BI in GERDA Phase II of about 4.6×10^{-4} cts/(keV kg year) (before) and 5.3×10^{-6} cts/(keV kg year) (after LAr veto). These values are well below the GERDA Phase II requirements [total BI $< 1 \times 10^{-3}$ cts/(keV kg year)].

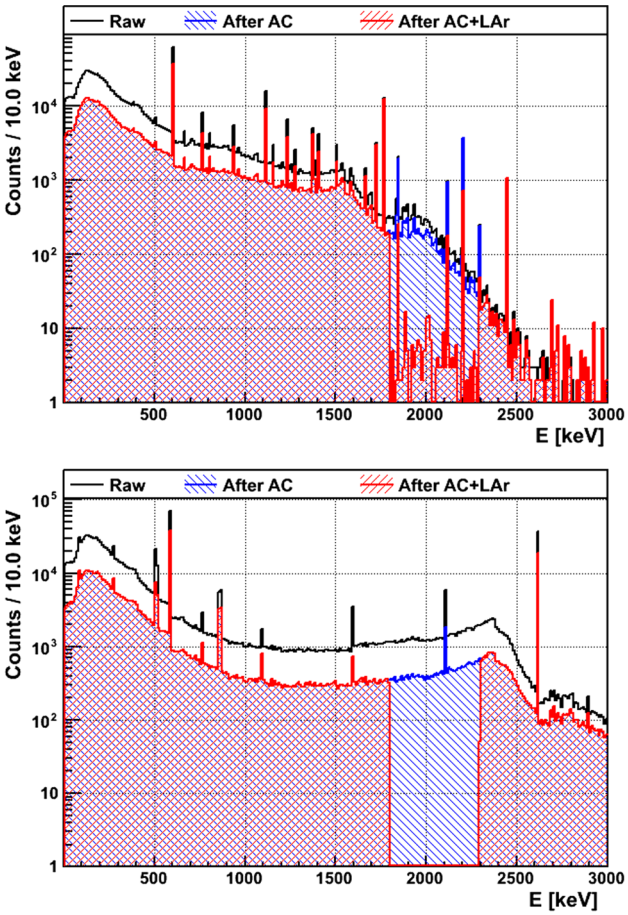

Fig. 5 Simulated energy spectra of germanium detector taken with ^{214}Bi (top) and ^{208}Tl (bottom) sources. The simulated spectra before cuts are shown in black, after the detector anti-coincidence (AC) in blue, and after applying the LAr scintillation veto cut in red [18]. Simulation of the anti-coincidence spectrum was only performed near $Q_{\beta\beta}$, to save computation time

2.3 Experimental setup

Detailed investigations of the ^{42}K background were performed in the LArGe test facility [8]. The scheme of the experimental setup is shown in Fig. 6. The setup allows to operate bare germanium detectors submerged in 1 m^3 of liquid argon. The cryostat is equipped with nine photomultiplier tubes (PMT) in order to suppress background events by detecting scintillation light in liquid argon, occurring in coincidence with germanium detector events (LAr veto). The LArGe setup is located at the Laboratori Nazionali del Gran Sasso (LNGS) Underground Laboratory at 3800 m w.e. depth. The achieved background index in LArGe [8] is close to the level of GERDA Phase I. Hence, an investigation of low background sources is possible.

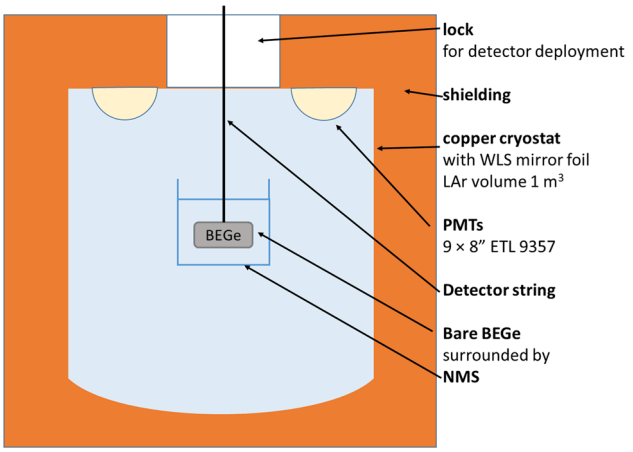

Fig. 6 Schematic view of the LArGe setup

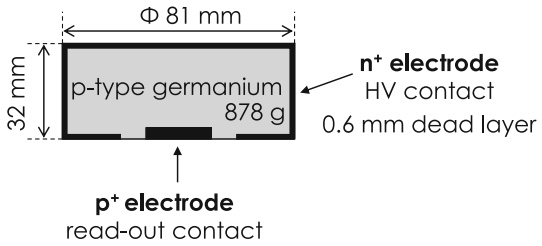

Fig. 7 Schematic drawing of the bare BEGe detector used in the study [23]

The measurements in LArGe were performed with a BEGe detector produced by Canberra [20]. A sketch of the detector and its dimensions are shown in Fig. 7. It is a p-type diode with the mass of 878 g. The thickness of the dead layer is estimated to be 0.6 mm. The detector mounting procedure and the holder design is the same as in GERDA Phase I [1], i.e. usage of low-mass and radio-pure materials close to the detector is implied. A GERDA Phase I custom made charge-sensitive preamplifier (CC2) with integrated J-FET transistor and RC feedback components is used for the signal conditioning [21]. Signals are digitized with a Flash-ADC (Struck SIS3301 VME, 14 bit, 100 MHz) card.

In order to enhance the ^{42}K signal, two ^{42}Ar sources with activities of (5.18 ± 0.91) Bq and (79 ± 15) Bq were produced by irradiating a cell filled with gaseous ^{nat}Ar at the accelerator operated in the Maier-Leibnitz Laboratory (MLL) of the Technische Universität München (TUM) via the reaction ^{40}Ar(^{7}Li,α p)^{42}Ar. The sources were introduced into the LArGe cryostat and homogeniously distributed in the liquid argon. With the enhanced signal rate from ^{42}K it is possible to investigate the behavior of ^{42}K ions and to test different background suppression methods with better counting statistics. The long measurement without NMS and measurement with a first version of the NMS were performed after the insertion of the source with lower activity. Measurements with the second, final version of the NMS, were done with both sources dissolved in liquid argon. The ^{42}Ar activity of these sources increased the count rate of the 1525 keV gamma peak (with respect to the measurements with natural argon) by factors of about 40 and 200, respectively. The increase is not exactly proportional to the source activity due to loss in dissolved activity caused by evaporation of liquid argon during refilling of the cryostat.

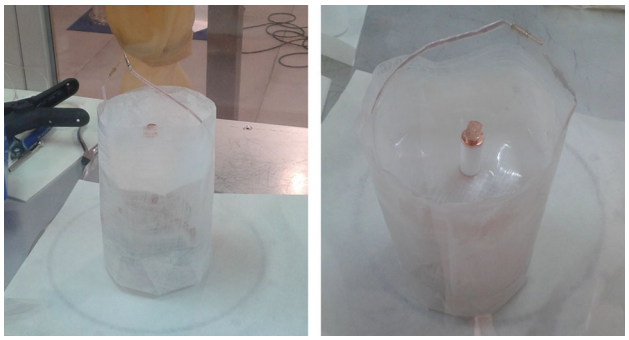

Fig. 8 Glued version of the NMS around the bare BEGe detector inside the glove box prior insertion into LArGe

3 Measurements of suppression factors

The energy region of 1540–3000 keV ("beta region") contains predominantly surface events from beta particles (see the ^{42}K decay scheme in Fig. 1) and overlaps the ROI at $Q_{\beta\beta} \pm 200$ keV. The energy region 1520–1530 keV mostly contains events from the 1525 keV gamma line.

The suppression factor (SF) in a certain energy region is expressed by the ratio of events in the unsuppressed (N_0) versus the suppressed (N_S) spectrum. For measurements with LAr veto, in order to be independent of the source strength, the LAr acceptance (ε_{LAr}) is taken into account. It is determined as the ratio of events from a pulse generator after and before LAr veto cut with an accuracy of about 1%. Hence,

$$SF = (N_0 - B_0) \cdot \varepsilon_{LAr} / (N_S - B_S), \quad (1)$$

with B_0 and B_S being the background levels before and after suppression, respectively.

3.1 Suppression of ^{42}K background by NMS

The BEGe detector inside the NMS (Fig. 8) was submerged in the LArGe cryostat. No deterioration of the detector's performance was found when operated with the NMS. A typical energy resolution of the detector is about 2.9 keV at the 2.6 MeV of the ^{208}Tl gamma line, similar to measurements without NMS. The energy spectra with and without NMS are shown in Fig. 9.

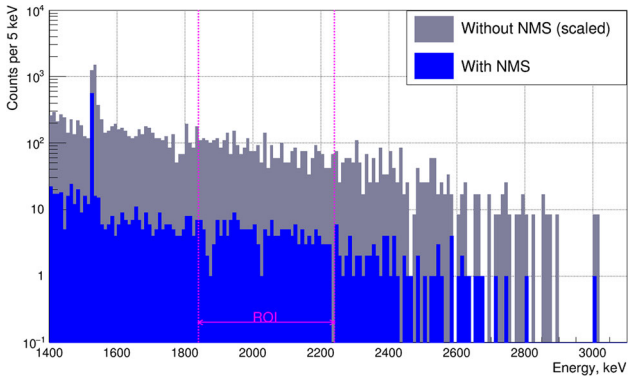

Fig. 9 Normalized energy spectra of the bare BEGe detector without NMS (grey area) and with NMS (blue)

Table 2 Count rates in the different energy regions with and without NMS. SF in the "beta region" is calculated taking into account a long-term decrease of the count rates (see Sect. 3.1 and Fig. 10)

	1520–1530 keV [cts/(kg day)]	1540–3000 keV [cts/(kg day)]
Without NMS	99 (10)	332 (18)
With NMS	29.0 (2.3)	17.1 (1.8)
SF		14.3 (2.1)

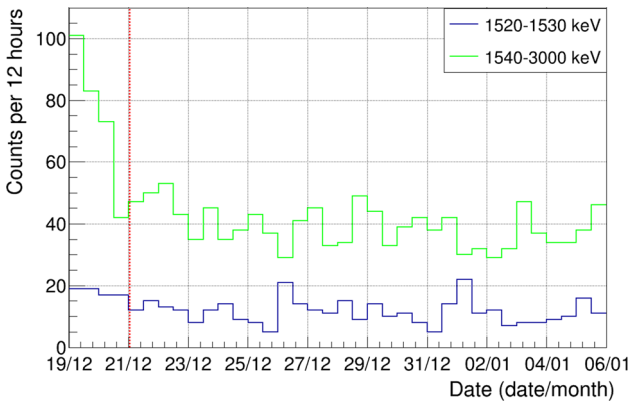

Fig. 10 Number of counts in the energy region 1520–1530 keV (blue) and 1540–3000 keV (green) in time for measurements of the detector without NMS in LArGe. The vertical red line indicates a period of the first 2 days which is not taken into account in the calculations

The energy spectra registered without and with NMS are scaled proportionally to the measurement time. Table 2 shows results from the calculation of the SF in the "beta region" using the ratio of count rates with and without NMS.
The first 2 days of data taking are not taken into account in order to reduce the influence of previously accumulated ^{42}K. An additional decrease of the ^{42}K count rate after first 2 days (see Fig. 10) is also accounted for in the calculation of the SF (henceforth referenced as "long-term correction").

Thus the SF is estimated to be 14.3 (2.1) with the uncertainty being dominated by counting statistics.

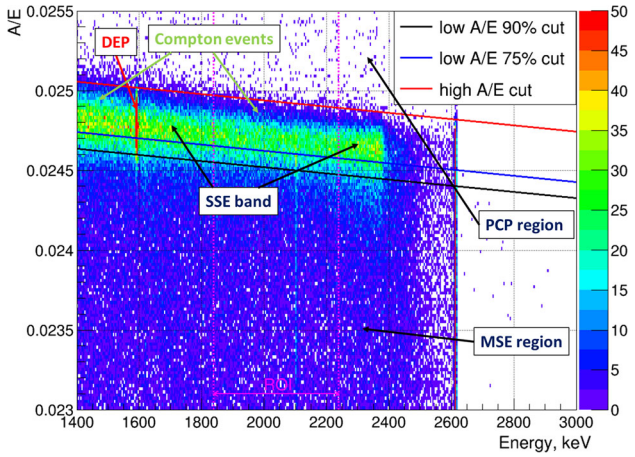

Fig. 11 Density diagram of the A/E parameter as a function of energy obtained in the measurements with the BEGe detector in LArGe with ^{228}Th source. Lines represent parameters of the PSD cuts obtained from this spectrum using events in the DEP and the Compton continuum

3.2 Suppression of ^{42}K background by PSD and LAr veto without NMS

A strong weighting potential close to the read-out electrode in the BEGe-type detectors enables a powerful pulse shape discrimination (PSD) of the acquired signals [22]. The PSD used in this work is based on the method described in [23]. It was developed for the discrimination between single-site events (SSE) and multi-site events (MSE) using differences in the amplitudes of current pulses with the same energy. The $0\nu\beta\beta$ events are expected to be SSE due to a rather short path of beta particles in the germanium detectors. In contrast, photons will often undergo several scatterings and are mostly MSE. Surface events exhibit a slower rising edge of the pulse due to diffusion of the electric charge into the n^+ surface (n^+ contact surface pulses, NSP). In consequence, these events have smaller amplitude to energy (A/E) ratio compared to events in the bulk of the detector. The events that deposit energy near the p^+ contact of the detector (p^+ contact pulses, PCP) have higher amplitudes than SSE, and they can be rejected as well.

The PSD cut parameters were determined from calibration data taken with a ^{228}Th source. Events in the double escape peak (DEP) of the 2.6 MeV gamma line of ^{208}Tl are predominantly single-site with a shape similar to $0\nu\beta\beta$ events. The low cut is usually determined in order to keep 90% of the events in the DEP. Figure 11 demonstrates such PSD cut obtained for the measurement with the BEGe detector in LArGe (rejected events are in the MSE region below the black line). The slope of the lines is determined from the distribution of the Compton scattering events. The p^+ events are rejected by applying a high cut (these events are above the

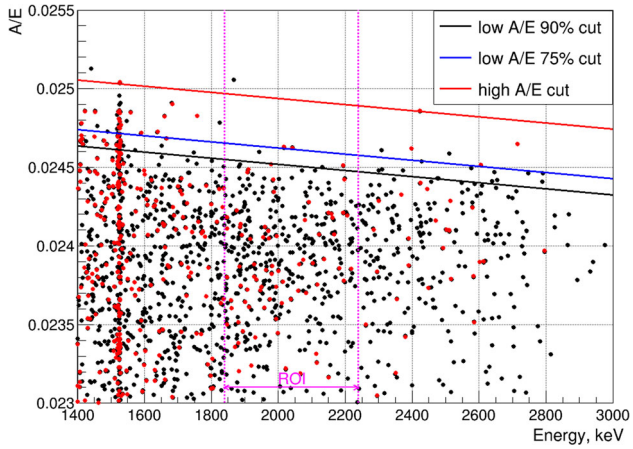

Fig. 12 A/E parameter versus the event energy registered by the BEGe detector in LArGe without NMS. Red dots indicate events removed by coincidence with the LAr veto. Here only the small ^{42}Ar source is dissolved in liquid argon

red line in Fig. 11). After applying low and high cuts 88% of the events remain in the DEP.

The first tests of ^{42}K suppression by PSD were performed with the bare BEGe detector in LArGe without a mini-shroud with the smaller activity ^{42}Ar source dissolved in liquid argon. The A/E distribution is shown in Fig. 12. The majority of events coming from the beta decay of ^{42}K are located below the SSE band. They are predominantly NSP from electrons which deposit their energy in the n^+ surface of the germanium detector. Only a small amount of the events is located in the SSE band.

The LAr veto is not very efficient in suppressing events from ^{42}K in the ROI, because such electrons often do not deposit much energy in liquid argon. However, combined PSD and LAr veto work efficiently, helping to suppress different types of background. The LAr veto acceptance ε_{LAr} measured by pulse generator is 96.5%. Part of the events in the SSE band is coming from other background sources (mostly from ^{228}Th). Such gamma background is removed with high probability by the scintillation veto [8]. After applying PSD and the LAr veto the events in the ROI are removed almost completely.

Table 3 summarizes the SFs in two energy ranges. Only two events survive from the initial 610 events in the ±200 keV window around the ROI of $0\nu\beta\beta$ after applying PSD and LAr veto. For a precise estimation of the ^{42}K SFs the remaining background sources have to be taken into consideration. Unfortunately, no measurements prior to dissolving of ^{42}Ar are available for this detector to estimate the background levels other than ^{42}K. So it is estimated with help of previous investigations with an encapsulated semi-coaxial germanium detector. The background level of that detector was $(0.12–4.6) \times 10^{-2}$ cts/(keV kg year) after LAr veto [8]. It was dominated by ^{208}Tl external to the cryostat, presumably

Table 3 Number of counts from the ^{42}K measurements and suppression factors in two energy regions, before and after applying different cuts for the BEGe detector without the NMS

	Energy region (keV)	
	1520–1530	1839–2239
		ROI
N_0 (events before cuts)	427	610
B_0 (other backgrounds)	0.9	23
N_S (after PSD + LAr veto)	10	2
B_S (other backgrounds)	0.015	0.62
SF	41.2	>121

from the PMTs [8], so we can expect to have this background with other detectors as well. In addition to this background, the contribution of cosmogenic background from ^{68}Ga in the BEGe detector is taken into account. The background index after applying the LAr veto and PSD is estimated from previous measurements in LArGe [8] and with help of simulations [18]. The accumulated statistics is not enough to precisely determine the suppression factor for ^{42}K background in the ROI, but it is possible to obtain a lower limit of >121 at 90% C.I. for the combined LAr veto and PSD cuts. This value is obtained using the TRolke class [24] assuming poisson statistics for the signal. The value can be improved by applying a stronger PSD cut: after applying a 73% PSD cut (low 75% and high cuts) no events survive the PSD veto (see Fig. 12).

It is necessary to notice that the suppression factor of the PSD depends on the detector performance: with worse A/E resolution some of the events can leak into the SSE band, reducing the efficiency of PSD cuts. That is why the PSD performance in LArGe may slightly differ from that in GERDA Phase II.

3.3 ^{42}K background suppression of NMS combined with PSD and LAr veto

The performance of the LAr veto with introduced NMS was investigated with a ^{228}Th source and with both ^{42}Ar sources dissolved in the liquid argon. The suppression factors of the LAr veto are obtained for the two versions of the NMS and without it (see Table 4).

The LAr veto suppression factors improve when using the NMS, which is clearly seen at the ^{42}K gamma line. The absorption length of light shifted by the NMS is much longer compared to the 128 nm scintillation light, and thus more light can reach the LAr veto light instrumentation. This may be a plausible reason for the enhanced performance of the LAr veto.

The combined performance of the NMS, PSD and LAr veto is scrutinized by ^{42}Ar measurements of the BEGe detec-

Table 4 Suppression by the LAr veto for the measurements with and without ^{228}Th sources. The spiked ^{42}Ar was present in all measurements

Energy regions (keV)	Suppression factors		
	Without NMS	Welded NMS	Glued NMS
Measurements without ^{228}Th source			
1520–1530	3.3 (4)	10.9 (1.1)	10.8 (1.3)
1839–2239	1.22 (10)	1.33 (12)	1.37 (16)
Measurements with external ^{228}Th			
1839–2239	26.8 (1.9)	37.2 (1.9)	31.9 (8)

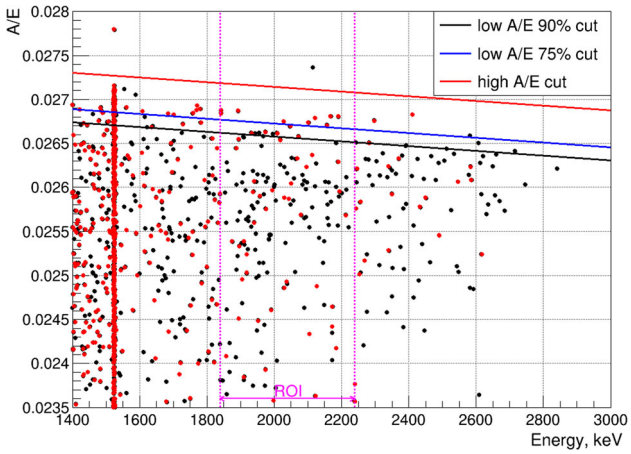

Fig. 13 A/E parameter versus the event energy registered by the BEGe detector in LArGe with NMS. Red dots indicate events removed by coincidence with the LAr veto. Both ^{42}Ar sources were used

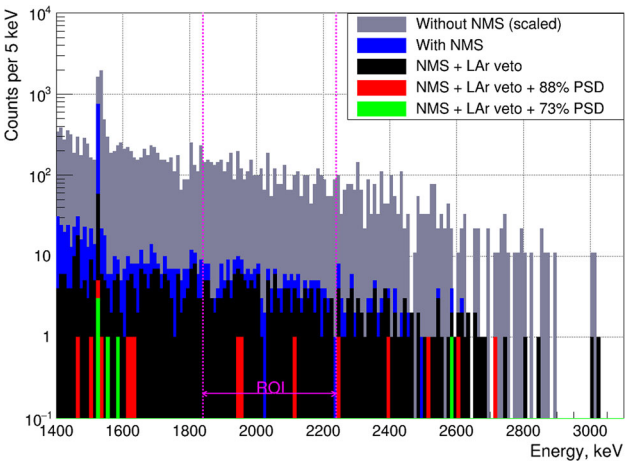

Fig. 14 Energy spectra demonstrating the suppression of ^{42}Ar events by the NMS and combined PSD and LAr cuts

Table 5 Number of counts from the ^{42}K measurement, before and after applying LAr veto and PSD cuts for the BEGe detector with the NMS

	Energy regions (keV)	
	1520–1530	1839–2239 ROI
N_0 (events before cuts)	750	216
B_0 (other backgrounds)	0.6	20
N_S (after PSD + LAr veto)	5	2
B_S (other backgrounds)	0.009	0.4
SF	144	>38

tor with the NMS. The A/E distribution measured with the ^{42}Ar source and with LAr veto is shown in Fig. 13.

In this measurement the final glued version of the NMS was implemented. Similarly to the previous measurements without NMS, most of the events coming from ^{42}K are rejected by PSD. The remaining part is removed by the LAr veto. The LAr veto allows to suppress events located in the SSE band more efficiently than those in the MSE band (see Fig. 13). This is an indication that at most a few of the events in the SSE band are electrons from ^{42}K. The number of events surviving PSD and LAr veto are shown in Table 5.

From the initial 216 events in the ROI only 2 events survive after applying LAr veto and PSD cuts. The estimated number of background events is 0.4. After taking into account the pulser acceptance, the SF is >38 (90% C.I.). By applying a stronger PSD cut (73%) it is possible to suppress all of the events.

Figure 14 shows the comparison of spectra with and without NMS and the effect of active ^{42}Ar suppression.

The gray area shows the spectrum of the bare BEGe detector without NMS scaled to the measurement time with the NMS. Other spectra demonstrate the ^{42}K suppression by the NMS and different cuts. In the scaled energy spectrum registered without the NMS there are 4384 events in ROI. After applying the PSD cut and the LAr veto only two events survive, including an estimated background of 0.4 events. Taking into account background components other than ^{42}K, the total suppression factor of NMS, LAr veto and PSD is higher than 513 at 90% C.I. (see Table 6).

The measurement with NMS has lower counting statistics compared to measurements without NMS. However, there is no indication that PSD performance in case of NMS is worse than in the measurements without NMS. In fact, it was found to be the same during ^{228}Th calibrations. Even though the LAr veto works slightly better with NMS, it almost does not

Table 6 Suppression factors in LArGe and estimated ^{42}K background rate for the GERDA Phase II setup before and after applying the LAr veto and PSD cuts

Experimental conditions	Suppression factor in LArGe	Expected ^{42}K background in ±200 keV ROI [10^{-3} cts/(keV kg year)]
No NMS	1	[210, 800][a]
NMS	14.3(2.1)	[13, 66]
PSD + LAr veto (no NMS)	>121	<[1.7, 7]
NMS + PSD + LAr veto	>513	<[0.4, 1.6]
NMS + PSD + LAr veto[b]	>1476	<[0.14, 0.5]

[a]Estimation is based on a simulation using a realistic range of dead layer thicknesses
[b]Estimation made with help of data taken without NMS, but with higher statistics

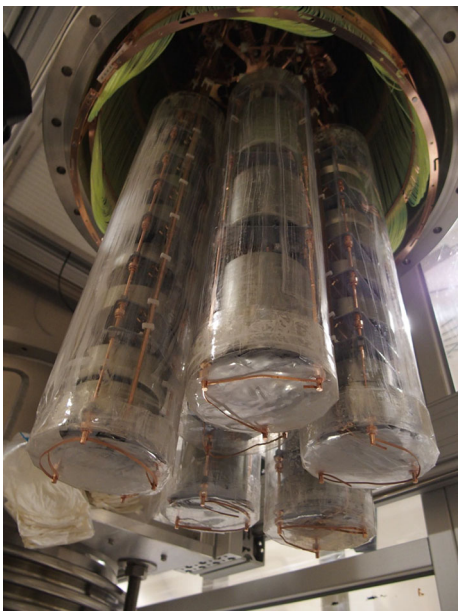

Fig. 15 Seven GERDA detector strings with the NMSs prior to insertion into the cryostat

suppress ^{42}K events in the ROI (see Table 4) and thus has little impact on the results. Therefore, it is safe to assume SF > 121 obtained in the measurement without NMS and better statistics (see Table 3) instead of SF > 38. With the NMS suppression factor of 14.3(2.1) using SF > 121 for PSD and LAr veto a total SF of > 1476 is obtained.

3.4 The NMS for GERDA Phase II

For each detector string in GERDA a dedicated NMS was prepared and mounted. A photo of the GERDA Phase II integration is shown in Fig. 15.

The setup was introduced into the GERDA cryostat and data taking was successfully started. The achieved background rate in GERDA Phase II after all cuts is approximately 1×10^{-3} cts/(keV kg year), satisfying desired specifications [25] and proving the effectiveness of the described concept of ^{42}Ar background suppression. Using SFs obtained in LArGe it is possible to estimate the ^{42}K background level in GERDA Phase II.

The expected ^{42}K background rate in GERDA is estimated by scaling the ^{42}Ar background in LArGe to GERDA using the ratio of the 1525 keV line intensities. The dead layer thickness has a big influence on the ^{42}K count rate in the ROI. That is why this factor is taken into consideration with the help of simulations. From these calculations it is expected that a bare BEGe detector in GERDA without a mini-shroud and before applying any cuts has a ^{42}K BI in the range of (2.1–8) $\times 10^{-1}$ cts/(keV kg year). The lower bound corresponds to a dead layer thickness of 1.0 mm with minimal expectation for the ^{42}K concentration in liquid argon, the higher value corresponds to 0.6 mm thickness and maximal expectation for the ^{42}K concentration. A typical value of the dead layer of a BEGe detector in GERDA is about 0.8 mm [3], so the limit for the ^{42}K background rate is expected to lay in the quoted range. By applying the SF derived in LArGe we obtain the background expectations in a simplified GERDA setup using NMS, PSD and LAr veto (see Table 6).

It is important to stress that although the estimated values in Table 6 demonstrate the general feasibility to suppress ^{42}Ar background to desired levels, they can not be viewed as an accurate prediction for the GERDA setup. GERDA has a total of 37 BEGe and coaxial detectors and a LAr veto system, which is rather different compared to LArGe . The difference in the LAr veto should not affect much the total suppression of the ^{42}K background due to its low ^{42}K suppression factor of ~ 1.2, compared to NMS and PSD performances (see Table 4). Also, some of the detectors in GERDA have an inferior PSD performance than the one tested in LArGe leading to a smaller suppression by PSD than expected. On the other hand, the suppression factors of the NMS in GERDA should be higher due to tight fitting of NMS and the detector strings.

In summary, the estimation allows to conclude that the combination of NMS and active ^{42}Ar background suppression techniques is capable to reach the GERDA Phase II background goal.

4 Conclusions

In this paper we show that the NMS is an efficient tool to suppress background caused by ^{42}K about fifteen times. Our measurements in LArGe also demonstrate that the performance of the LAr veto is slightly enhanced by the NMS. PSD proofs to be a very good method to mitigate surface events from ^{42}K decays. A combination of a NMS with the active background suppression methods PSD and LAr veto allows

to suppress ^{42}K background in LArGe by more than three orders of magnitude.

The glued NMS is easy to construct and robust enough for handling and mounting. The NMS is made from radiopure material with an expected contribution to the background index of only 4.6×10^{-4} cts/(keV kg year) and 5.3×10^{-6} cts/(keV kg year) before and after the LAr scintillation veto, respectively. These values are well below the requirements for GERDA Phase II and may also be acceptable for future experiments.

The NMSs were successfully mounted and immersed into the liquid argon cryostat of GERDA. The feasibility and performance of the described concept of ^{42}Ar suppression is proven. We estimate the possible level of background from ^{42}K in GERDA Phase II to be $<[0.14,0.5] \times 10^{-3}$cts/(keV kg year) with NMS and after applying PSD and LAr veto cuts in the ROI, taking into account simulations and the results obtained in LArGe . This limit already meets the Phase II design criterion of BI$< 1 \times 10^{-3}$cts/(keV kg year) and can be further improved by a stronger PSD cut or by using detectors with thicker dead layers.

Acknowledgements We would like to thank F. Calaprice from the Princeton University for providing us the nylon. A special thank to Maria Laura di Vacri and Stefano Nisi from LNGS, for their involvement in the searches for radiopure components. Big thank to Bernhard Schwingenheuer for many suggestions and discussions. The investigations were supported by the Max Planck Society (MPG), the German Research Foundation (DFG) via the Excellence Cluster Universe, the Italian Istituto Nazionale di Fisica Nucleare (INFN), the Swiss National Science Foundation (SNF), the Russian Foundation for Basic Research RFBR (Grant 16-02-01096), the Polish National Science Centre (Grant No. UMO-2012/05/E/ST2/02333) and the Foundation for Polish Science (Grant No. TEAM/2016-2/17).

Funded by SCOAP[3].

References

1. The GERDA Collaboration, Eur. Phys. J. C **73**, 2330 (2013)
2. CANBERRA Broad Energy Ge (BEGe) Detector, http://www.canberra.com/products/485.asp
3. The GERDA Collaboration, Eur. Phys. J. C **74**, 2764 (2014)
4. B.J. Mount et al., Phys. Rev. C **81**, 032501 (2010)
5. R.B. Firestone, *Table of Isotopes*, 8th edn. (Wiley, New York, 1998)
6. V.D. Ashitkov et al., Instrum. Exp. Tech. **46**, 153160 (2003)
7. A.S. Barabash et al., J. Phys. Conf. Ser. **718**, 062004 (2016)
8. M. Heisel et al., Eur. Phys. J. C **75**, 506 (2015)
9. K. Pelczar, Backgrounds in the GERDA and DarkSide Experiments. Radioactive Ions in Cryogenic Liquids, PhD thesis, Jagiellonian University, Kraków (2016)
10. J. Benziger et al., Nucl. Instrum. Methods **A582**, 509–534 (2007)
11. L. Cadonati, The Borexino Solar Neutrino Experiment and its Scintillator Containment Vessel, PhD thesis (2001)
12. http://www.sigmaaldrich.com/catalog/product/aldrich/185213?lang=en&region=RU
13. P. Peiffer, Liquid argon as active shielding and coolant for bare germanium detectors: a novel background suppression method for the GERDA $0\nu\beta\beta$ experiment, PhD thesis (2007)
14. L. Baudis et al., J. Instrum. (JINST) **10**, P09009 (2015)
15. A. Pocar, Low Background Techniques and Experimental Challenges for Borexino and its Nylon Vessels, PhD thesis, Princeton University (2003)
16. M.L. di Vacri et al., AIP Conf. Proc. **1672**, 150001 (2015)
17. M. Boswell et al., IEEE Trans. Nucl. Sci. **58**, 1212 (2011)
18. B. Lehnert, Search for $2\nu\beta\beta$ Excited State Transitions and HPGe Characterization for Surface Events in GERDA Phase II, PhD thesis (2016)
19. M. Agostini et al., Eur. Phys. J. C. arXiv:1711.01452
20. http://www.canberra.com/products/485.asp
21. S. Riboldi et al., Procs. IEEE Nuclear Science Symposium and Int. Workshop on Room Temperature Semiconductor Detectors, p. 1386 (2010)
22. M. Agostini et al., J. Instrum. (JINST) **6**, P03005 (2011)
23. D. Budjáš et al., J. Instrum. (JINST) **4**, P10007 (2009)
24. J. Lundberg et al., Comput. Phys. Commun. **181**, 683–686 (2010)
25. The GERDA collaboration, Nature **544**, 47 (2017)